

Communicating with Large Intelligent Surfaces: Fundamental Limits and Models

Davide Dardari, *Senior Member, IEEE*

Abstract

This paper analyzes the fundamental communication problem involving large intelligent surfaces (LIS) starting from electromagnetic (e.m.) arguments. Since the numerical solution of the corresponding optimal eigenfunction problem is in general computationally prohibitive, simple but accurate analytical expressions for the link gain and available degrees-of-freedom (DoF) are derived. It is shown that the achievable DoF and gain offered by the wireless link are determined only by geometric factors, and that the classic Friis' formula is no longer valid in this scenario where transmitter and receiver could operate in the near-field regime. Furthermore, results indicate that, contrarily to classic MIMO systems, when using LIS one can exploit all the potentially available DoF even in LOS conditions, which corresponds to a drastic increase of spatial capacity density.

Index Terms

Large intelligent surfaces; meta-surfaces; wireless communication; fundamental limits; degrees of freedom

I. INTRODUCTION

Future wireless networks are expected to become distributed intelligent communication, sensing and computing entities. This will allow to meet ultra-reliability, high capacity densities, extremely low-latency and low-energy consumption requirements posed by emerging application scenarios such as that of Industrial Internet of Things in Factories of the Future [1]. The current trend to satisfy part of such requirements is through cell densification, massive multiple-input multiple-output (MIMO) transmission, and the exploitation of higher frequency bands (e.g., millimeter and THz) [2]. Unfortunately, when moving to higher frequency

D. Dardari is with the Dipartimento di Ingegneria dell'Energia Elettrica e dell'Informazione "Guglielmo Marconi" (DEI), CNIT, University of Bologna, Cesena Campus, Cesena (FC), Italy, (e-mail: davide.dardari@unibo.it).

Part of this work has been submitted to the International Conference on Communication ICC 2020.

bands the channel path-loss increases and the multipath becomes sparse so that the spatial multiplexing peculiarity of MIMO, i.e., the channel degrees-of-freedom (DoF), guaranteed at lower frequencies by rich multipath, is lost in favor of only beamforming gain, which increases the communication capacity only logarithmically with the number of antennas [3].

Recently, the introduction of programmable meta-surfaces to realize, for instance, smart electromagnetic (e.m.) reflectors, large configurable antennas, using thin meta-materials has opened new very appealing perspectives [4]–[7]. In fact, with meta-materials e.m. waves can be shaped almost arbitrarily. These *intelligent surfaces* can be embedded in daily life objects such as walls, clothes, buildings, etc., and can be used as distributed platforms to perform low-energy and low-complexity sensing, storage and analog computing. Environments coated with intelligent surfaces constitute the recently proposed *smart radio environments* concept [8]–[10]. In smart radio environments, the design paradigm has changed from wireless devices/networks that adapt themselves to the environment (e.g., propagation conditions), to the joint optimization of both devices and environment using reconfigurable intelligent surfaces (RISs) with the purpose to move toward the ultimate limits of wireless communications.

This new technology and paradigm change provides much more DoF in network design as well as the potential to achieve the goals of next generation wireless networks, but it has also opened several fundamental questions that are still unsolved, such as understanding the theoretical limits of smart radio environments and how to achieve them. In addition, new unconventional modeling, analysis and design tools are needed to optimize their performance.

In this context, most of papers deal with intelligent surfaces used to assist multipath propagation, i.e., as reconfigurable reflectors [8]. Along a different direction, in [11] a general theory of space-time modulated digital coding meta-surfaces to obtain simultaneous manipulations of e.m. waves in both space and frequency domains is proposed and validated in the far-field regime. Less papers analyze the potential of using meta-surfaces as large intelligent surface (LIS) antennas [12]. LIS (e.g., on walls), medium intelligent surface (MIS) (e.g., on cars/truck), and small intelligent surface (SIS) (e.g., on smartphones/sensors), provide a great opportunity to move towards the ultimate capacity limit of the wireless channel.

When considering LIS, classic models for antenna arrays fail to capture the actual wireless link characteristics in terms of gain, path-loss and available DoF as they assume (Fraunhofer) far-field condition (i.e., distance much larger than the antenna dimension so that waves can be considered plane [13]), whereas with LIS the size of the antenna becomes comparable to the distance of the link (near-field regime). Moreover, they usually do not account for the

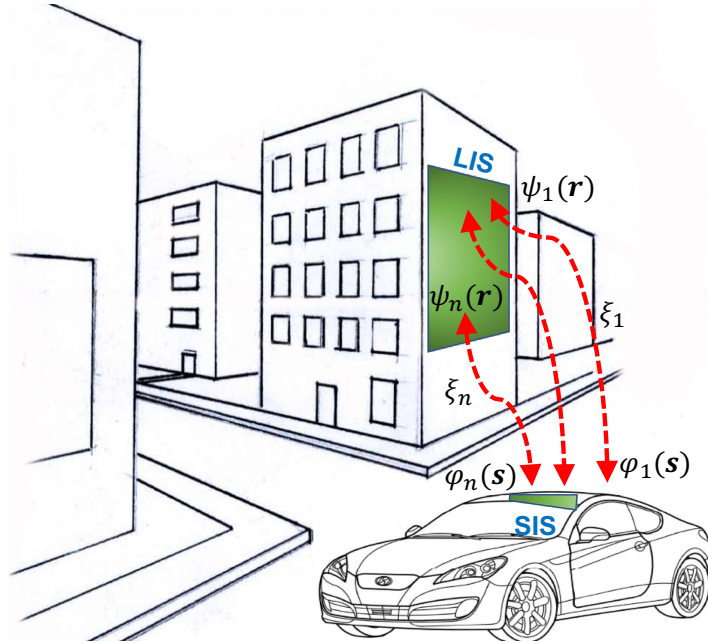


Fig. 1. Example of LIS-based communication scenario.

flexibility in generating the current distribution offered by LIS and hence common results of aperture antennas are no longer valid. Therefore, new models based on the ultimate physical limitation brought by the e.m. transportation of information should be considered. The main fundamental results on e.m. transportation of information can be found in [14] and references therein. These results mainly address the computation of the spatial dimensionality of the e.m. when considering finite volumes with sources and scatterers in the far-field, but they do not consider the DoF available in a communication system employing intelligent surfaces [15]–[17]. One of the earliest work using LIS is [12], which considers the communication between a single-antenna user with a LIS, where a capacity analysis is presented.

In this paper, the optimal communication between LIS/SIS is addressed as an eigenfunction problem starting from an e.m. formulation. To obtain high-level descriptions of LIS-based communication and to avoid extensive and sometimes prohibitive e.m.-level simulations, simple but accurate analytical expressions for the link gain and the available orthogonal communication modes (i.e., DoF) between transmitter and receiver are derived. These expressions allow to get important insights about the communication between intelligent surfaces and can serve as design guidelines in future wireless networks employing LIS.

When moving towards high frequencies, line-of-sight (LOS) communication becomes predominant and multipath weaker. We show that, contrarily to classic MIMO results, with

LIS the available DoF can be larger than one without the exploitation of multipath, thus boosting in principle the channel capacity. In addition, the achievable DoF and gain offered by the wireless link are shown to be determined only by geometric factors normalized to the wavelength, and that the classic Friis' formula is no longer valid when using LIS.

Notation and definitions: Lowercase bold variables denote vectors in the 3D space, i.e., $\mathbf{r} = \mathbf{u}_x \cdot r_x + \mathbf{u}_y \cdot r_y + \mathbf{u}_z \cdot r_z$ is a vector with cartesian coordinates (r_x, r_y, r_z) , $\hat{\mathbf{r}}$ is a unit vector denoting its direction, and $r = |\mathbf{r}|$ denotes its magnitude, where $\hat{\mathbf{u}}_x$, $\hat{\mathbf{u}}_y$ and $\hat{\mathbf{u}}_z$ represent the unit vectors in the x , y and z directions, respectively. Italic capital letters (e.g., $E(\mathbf{r})$, $J(\mathbf{r})$) represent electromagnetic vector functions. Boldface capital letters are matrices (e.g., \mathbf{H}), where \mathbf{I} is the identity matrix, and \dagger indicates the conjugate transpose operator. $\nabla^2 J(\mathbf{r})$ is the Laplacian of the vector function $J(\mathbf{r})$. Surfaces and volumes are indicated with calligraphic letters \mathcal{S}_T , where $A_T = |\mathcal{S}_T|$ is their Lebesgue measure. Define the \mathcal{L}_2 -norm $\|\mathbf{r}\|$, the Frobenius norm $\|\mathbf{X}\| = \sqrt{\sum_{k=1}^N \sum_{j=1}^N |\{\mathbf{X}\}_{kj}|^2}$, and the outer product (tensor product) $\mathbf{r} \otimes \mathbf{s}$, where $\{\mathbf{r} \otimes \mathbf{s}\}_{kj} = r_k s_j$, and $\{\mathbf{X}\}_{kj}$ is the kj th element of matrix \mathbf{X} . Moreover, denote with μ , ϵ , and $\eta = \sqrt{\mu/\epsilon}$ the permittivity, permeability and impedance of free-space, respectively, and c the speed-of-light.

II. GENERAL PROBLEM FORMULATION

Thanks to the adoption of meta-materials, with LIS one can synthesize in principle any current distribution, then it is of interest to investigate how many orthogonal channels, i.e., communication modes or DoF, are possible when two LIS/SIS are communicating with each other. To this purpose, we approximate the intelligent surface as a continuous array of an infinite number of infinitesimal antennas.

A. Problem Formulation

Consider a transmit MIS/SIS antenna with surface \mathcal{S}_T of area $A_T = |\mathcal{S}_T|$ containing e.m. monochromatic source currents with Fourier representation $J(\mathbf{s}, \omega)$, with ω being the angular frequency, different from zero in $\mathbf{s} \in \mathcal{S}_T$, which generate an electric field $E(\mathbf{r}, \omega)$ in free-space, and a receive LIS antenna \mathcal{S}_R not intersecting \mathcal{S}_T , with area $A_R = |\mathcal{S}_R|$.¹ Due to the reciprocity of the radio medium, their role can be exchanged.

¹Here we consider only surfaces because of their higher practical relevance, even though most of the following results can be extended to volumes as well.

Each frequency component satisfies the inhomogeneous Helmholtz wave equation²

$$\nabla^2 E(\mathbf{r}) + k_0^2 E(\mathbf{r}) = jk_0 \eta J(\mathbf{r}), \quad (1)$$

where $k_0 = \omega/c = 2\pi/\lambda$ is the wavenumber, λ the wavelength, and we have dropped the explicit dependence on ω to lighten the notation.

Any point source in \mathcal{S}_T generates the (outgoing) wave given by the tensor Green's function [13]

$$G(\mathbf{r}) = -\frac{j\omega\mu}{4\pi} \left[\mathbf{I} + \frac{1}{k_0} \nabla \nabla \right] \frac{\exp(-jk_0 r)}{r}, \quad (2)$$

with $r = |\mathbf{r}|$, which obeys the Helmholtz equation.

By expanding (2) it is [19]

$$\begin{aligned} G(\mathbf{r}) = & -\frac{j\eta \exp(-jk_0 r)}{2\lambda r} \left[\left(\mathbf{I} - \hat{\mathbf{r}} \cdot \hat{\mathbf{r}}^\dagger \right) + \frac{j\lambda}{2\pi r} \left(\mathbf{I} - 3\hat{\mathbf{r}} \cdot \hat{\mathbf{r}}^\dagger \right) \right. \\ & \left. - \frac{\lambda^2}{(2\pi r)^2} \left(\mathbf{I} - 3\hat{\mathbf{r}} \cdot \hat{\mathbf{r}}^\dagger \right) \right] \simeq -\frac{j\eta \exp(-jk_0 r)}{2\lambda r} \left(\mathbf{I} - \hat{\mathbf{r}} \cdot \hat{\mathbf{r}}^\dagger \right) \end{aligned} \quad (3)$$

where we grouped the terms multiplying, respectively, the factors $1/r$, $1/r^2$ and $1/r^3$. It is evident from (3) that when $r \gg \lambda$, the second and third terms can be neglected and hence the right-hand side approximation in (3) holds.³ By adding all the waves from the sources in \mathcal{S}_T , the resulting wave in \mathbf{r} is

$$E(\mathbf{r}) = \int_{\mathcal{S}_T} G(\mathbf{r} - \mathbf{s}) J(\mathbf{s}) d\mathbf{s}. \quad (4)$$

The goal is to determine how many orthogonal waves, namely DoF, can be activated between \mathcal{S}_T and \mathcal{S}_R , as well as the corresponding coupling intensity. To determine the dimensionality of the waves, one has to solve the following coupled eigenfunction problem [20], [21]

$$\xi^2 J(\mathbf{s}) = \int_{\mathcal{S}_T} K_T(\mathbf{s}, \mathbf{s}') J(\mathbf{s}') d\mathbf{s}' \quad (5)$$

$$\xi^2 E(\mathbf{r}) = \int_{\mathcal{S}_R} K_R(\mathbf{r}, \mathbf{r}') E(\mathbf{r}') d\mathbf{r}', \quad (6)$$

where

$$K_T(\mathbf{s}, \mathbf{s}') = \int_{\mathcal{S}_R} G^\dagger(\mathbf{r} - \mathbf{s}) G(\mathbf{r} - \mathbf{s}') d\mathbf{r} \quad (7)$$

$$K_R(\mathbf{r}, \mathbf{r}') = \int_{\mathcal{S}_T} G(\mathbf{r} - \mathbf{s}) G^\dagger(\mathbf{r}' - \mathbf{s}) d\mathbf{s}. \quad (8)$$

²Similar formulation can be done for the magnetic field in case of magnetic currents even though it is always possible to model the problem using equivalent source currents [18].

³Under this condition the system does not work in the 'reactive' near-field.

Since $K_T(\mathbf{s}, \mathbf{s}')$ and $K_R(\mathbf{r}, \mathbf{r}')$ are Hermitian kernels, a set of eigenfunctions $\{\phi_n(\mathbf{r})\}$, $\{\psi_n(\mathbf{s})\}$ with real eigenvalues ξ_1^2, ξ_2^2, \dots , solution of (5) and (6) exists. Specifically, any current density and wave in \mathcal{S}_T and \mathcal{S}_R can be written, respectively, as

$$J(\mathbf{r}) = \sum_n a_n \phi_n(\mathbf{r}) \quad E(\mathbf{r}) = \sum_n b_n \psi_n(\mathbf{r}), \quad (9)$$

where $\{\phi_n(\mathbf{r})\}$ and $\{\psi_n(\mathbf{r})\}$ are two sets of orthonormal (vector) functions that are complete, respectively, in \mathcal{S}_T and \mathcal{S}_R , i.e.,

$$\int_{\mathcal{S}_T} \phi_n(\mathbf{r}) \phi_m^\dagger(\mathbf{r}) d\mathbf{r} = \delta_{nm} \quad \int_{\mathcal{S}_R} \psi_n(\mathbf{r}) \psi_m^\dagger(\mathbf{r}) d\mathbf{r} = \delta_{nm}. \quad (10)$$

Each solution is a spatial dimension of the system across which one can establish an orthogonal communication (see Fig. 1). Since the surfaces \mathcal{S}_T and \mathcal{S}_R are finite, in practice the number of dimensions, i.e., the number of eigenvalues ξ_n^2 different from zero, is finite.

The geometric interpretation is that the generic source current $J(\mathbf{s})$ can be projected onto the coordinate system determined by the orthogonal (vector) eigenfunctions $\{\phi_n(\mathbf{s})\}$ then, through the tensor $G(\mathbf{r})$ in (4), the n th eigenfunction $\phi_n(\mathbf{s})$ of surface \mathcal{S}_T is put in one-to-one correspondence with the n th eigenfunction $\psi_n(\mathbf{r})$ of the receive surface \mathcal{S}_R through the scaling singular value ξ_n . Therefore, if one takes as source function the n th eigenfunction, i.e., $J(\mathbf{s}) = \phi_n(\mathbf{s})$, $\mathbf{s} \in \mathcal{S}_T$, then the output electric field results $\xi_n \psi_n(\mathbf{r})$, $\mathbf{r} \in \mathcal{S}_R$. In general it is $b_n = \xi_n a_n$.

The eigenfunction decomposition ensures the maximum level of coupling between the sources in \mathcal{S}_T and the field in \mathcal{S}_R , so that the intensity of the electric field $E(\mathbf{r})$ within \mathcal{S}_R , $\int_{\mathcal{S}_R} \|E(\mathbf{r})\|^2 d\mathbf{r}$, is maximized.

In terms of communication system representation, the eigenfunction decomposition leads to the optimal communication architecture depicted in Fig. 2. From it we obtain the input-output representation in terms of D parallel channels

$$y_n = \xi_n x_n + w_n, \quad i = 1, 2, \dots, D, \quad (11)$$

being w_n is the additive white Gaussian noise (AWGN), where the D input data streams $\{x_n\}$ are recovered at the receiver after the convolution of the received signal $E(\mathbf{r})$ with the appropriate basis functions $\{\phi_n(\mathbf{s})\}$. This scheme is information-theoretically optimal.

It is worthwhile to highlight that the capacity gain with respect to $D = 1$ for a given signal-to-noise ratio (SNR) could be significant. For example, supposing uniform power allocation, such gain is

$$G_C = \frac{D \log_2 \left(1 + \frac{\text{SNR}}{D} \right)}{\log_2 (1 + \text{SNR})}. \quad (12)$$

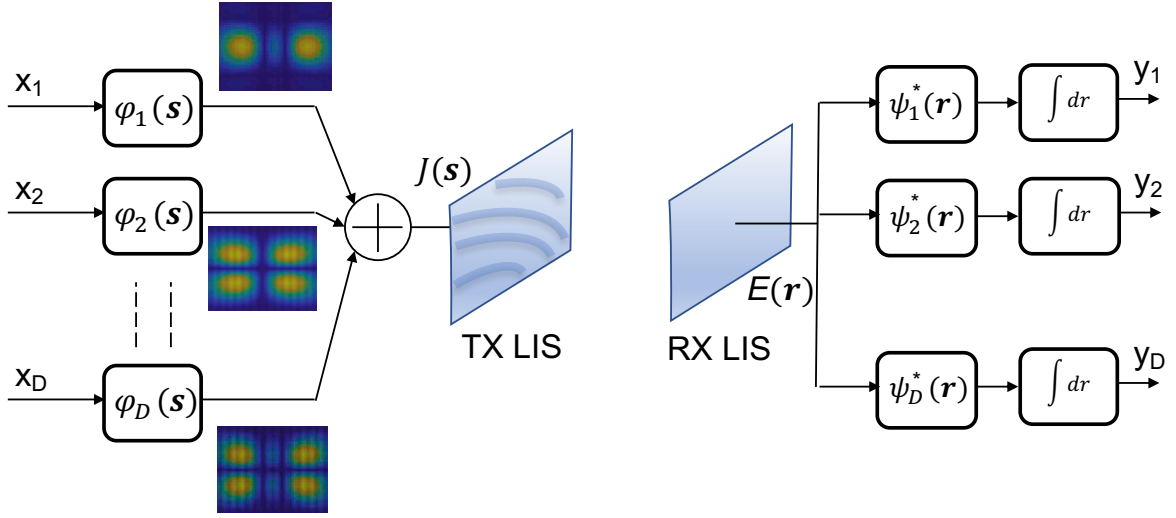


Fig. 2. Communication architecture based on orthogonal parallel channels.

B. Maximum Coupling Intensity Between Intelligent Surfaces

The effect of each polarization direction can be studied separately if the components of $J(\mathbf{s}) = J_x(\mathbf{s})\hat{\mathbf{u}}_x + J_y(\mathbf{s})\hat{\mathbf{u}}_y + J_z(\mathbf{s})\hat{\mathbf{u}}_z$ are taken orthogonal. Therefore, without of generality, suppose we excite the x -component, i.e., $J(\mathbf{s}) = J_x(\mathbf{s})\hat{\mathbf{u}}_x$. By exploiting the identity (35) in Appendix A and considering the last term of (3), the total (dimensionless normalized) coupling factor between intelligent surfaces results

$$\begin{aligned} c_x &= \frac{(4\pi)^2}{\lambda^2} \frac{1}{(\omega\mu)^2} \sum_n \xi_n^2 = \frac{4}{\eta^2} \int_{S_R} \int_{S_T} \|G_x(\mathbf{r} - \mathbf{s})\|^2 d\mathbf{r} d\mathbf{s} \\ &= \frac{1}{\lambda^2} \int_{S_R} \int_{S_T} \frac{(r_y - s_y)^2 + (r_z - s_z)^2}{|\mathbf{r} - \mathbf{s}|^4} d\mathbf{r} d\mathbf{s}. \end{aligned} \quad (13)$$

The notation $G_x(\cdot)$ indicates we consider only the first column of tensor $G(\cdot)$, corresponding to the contribution caused by an excitation in the x -direction. Note that in general the excitation in the x -direction might contribute to all directions in the received electric field. The expressions for the other exciting directions are similar with mutual exchange of x , y and z .

In [20] the approximate solution to the eigenfunction problem valid for two collinear rectangular prisms at distance d oriented along the z -axis of size $V_T = \Delta x_T \Delta y_T \Delta z_T$ and $V_R = \Delta x_R \Delta y_R \Delta z_R$, respectively, is presented. Specifically, the solution holds when the volumes are far apart compared to their sizes, i.e., $d \gg \Delta x_T, \Delta y_T, \Delta z_T, \Delta x_R, \Delta y_R, \Delta z_R$, which means the

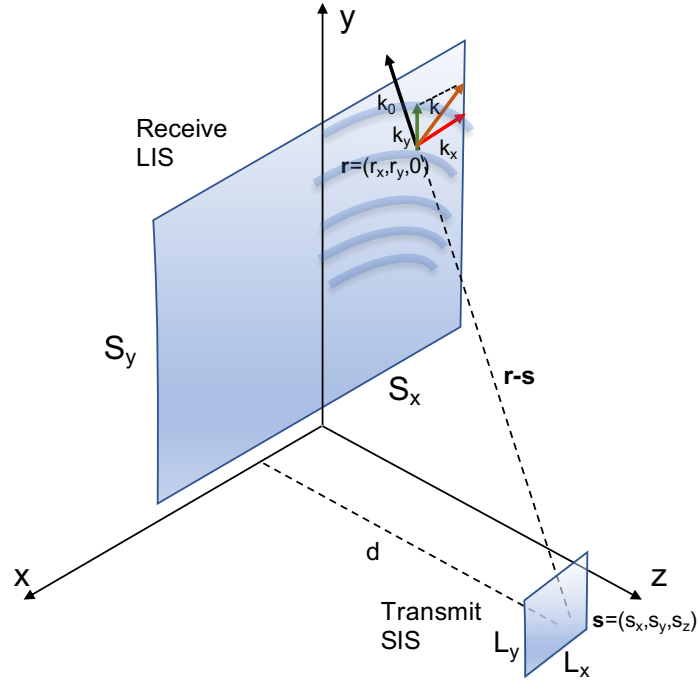


Fig. 3. Geometric configuration between SIS and LIS.

(Fraunhofer) far-field region. In this case, the DoF available for communication have been found to be

$$D = \frac{\Delta x_T \Delta y_T \Delta x_R \Delta y_R}{d^2 \lambda^2}, \quad (14)$$

whereas the total (un-normalized) coupling factor is

$$c \propto \frac{V_T V_R}{(4\pi d)^2}. \quad (15)$$

Note that the thickness of volumes in the z axis does not affect the DoF but only the gain.

Incidentally, for very small antennas, $\Delta x_T \Delta x_R \ll d \lambda$, $\Delta y_T \Delta y_R \ll d \lambda$, only one solution to the eigenfunctions problem exists, corresponding to a plane wave that travels with direction from the transmit antenna to the receive antenna. Unfortunately, the result above by [20] is no longer valid when analyzing LIS as the assumption of far apart antennas, and hence the parallax approximation typical of the Fraunhofer region, do not hold anymore.

The analytical derivation of the eigenfunctions and eigenvalues in general is elusive and one has to resort to e.m. simulations, which could be prohibitive for LIS and typically they do not provide general insights. In the next sections we bypass the direct derivation of the solutions of the eigenfunction problem by resorting to geometric arguments, with the purpose

to determine the DoF available for communication. Our aim is to derive simple expressions for LIS in particular geometric configurations of interest, also valid in the radiating near-field.

III. POWER GAIN BETWEEN LARGE AND SMALL-MEDIUM INTELLIGENT SURFACES

The coupling intensity for any generic geometric configuration of antennas can be easily obtained by solving (13) numerically. Nevertheless, closed-form expressions can be obtained for some relevant cases from which some interesting insights can be deduced.

Consider a transmit MIS/SIS and a receive LIS at distance d . This is expected to be a common situation in practice where the MIS/SIS antenna might be embedded, for instance, into a smartphone or on top of a car, whereas the LIS coats a wall of a building. Without loss of generality, the receive LIS is deployed along the xy -plane at $z = 0$, therefore the generic point on the surface is represented by the coordinates $\mathbf{r} = (r_x, r_y, 0) \in \mathcal{S}_R$ (see Fig. 3). Denote with $\mathbf{s} = (s_x, s_y, s_z) \in \mathcal{S}_T$ the coordinates of the generic point source of the transmit surface \mathcal{S}_T . The centers and sizes of the transmit and receive intelligent surfaces are, respectively, $\mathbf{s}_0 = (x_0, y_0, d)$, (L_x, L_y) and $(0, 0, 0)$, (S_x, S_y) . The corresponding areas are $A_T = L_x L_y$ and $A_R = S_x S_y$. Since the transmit antenna is a MIS/SIS, it is reasonable to assume that $L_x, L_y \ll d$, $L_x \ll S_x$, and $L_y \ll S_y$.

To calculate the power gain between the transmit SIS and the receive LIS, one has to consider only the component in (13) perpendicular to the surface, i.e.,

$$\begin{aligned} g &= \frac{1}{\lambda^2} \int_{\mathcal{S}_R} \int_{\mathcal{S}_T} \frac{(r_y - s_y)^2 + (r_z - s_z)^2}{|\mathbf{r} - \mathbf{s}|^4} \hat{\mathbf{p}} \cdot \hat{\mathbf{n}} \, d\mathbf{r} \, ds \\ &\simeq \frac{A_T}{\lambda^2} \int_{\mathcal{S}_R} \frac{((r_y - y_0)^2 + d^2) \, d}{|\mathbf{r} - \mathbf{s}_0|^5} \, d\mathbf{r}, \end{aligned} \quad (16)$$

where $\hat{\mathbf{p}} = (\mathbf{r} - \mathbf{s})/|\mathbf{r} - \mathbf{s}|$, and $\hat{\mathbf{n}} = \hat{\mathbf{z}}$. In (16), we have made the approximations $s_z \simeq d$ and $|\mathbf{r} - \mathbf{s}|^2 \simeq |\mathbf{r} - \mathbf{s}_0|^2$, since the transmit antenna is small compared to the distance d . As a consequence, the result does not depend on SIS orientation but only on its area A_T . Equation (16) can be solved in closed-form but the final expression is quite long and it does not provide important insights. For the sake of space, we report here the result valid for $\mathbf{s}_0 = (0, 0, d)$ from which some interesting conclusions can be drawn. In this case, (16) becomes

$$\begin{aligned} g &= \frac{A_T}{\lambda^2} \int_{-S_x/2}^{S_x/2} \int_{-S_y/2}^{S_y/2} \frac{d (r_y^2 + d^2)}{(r_x^2 + r_y^2 + d^2)^{5/2}} \, dr_x \, dr_y \\ &= \frac{4d A_T S_x}{3\lambda^2} \int_{-S_y/2}^{S_y/2} \frac{6d^2 + S_x^2 + 6r_y^2}{(d^2 + r_y^2) (4d^2 + S_x^2 + 4r_y^2)^{3/2}} \, dr_y, \end{aligned} \quad (17)$$

which gives

$$g = \frac{8A_T}{3\lambda^2} \left(\frac{S_x S_y d}{(S_x^2 + 4d^2) \sqrt{S_x^2 + S_y^2 + 4d^2}} + \tan^{-1} \left(\frac{S_x S_y}{2d \sqrt{S_x^2 + S_y^2 + 4d^2}} \right) \right). \quad (18)$$

For square LIS, the last expression simplifies as follows

$$g = \frac{4A_T}{3\lambda^2} \left(\frac{\sqrt{2F}}{\sqrt{1 + 2F}(1 + 4F)} + 2\text{acot} \left(\sqrt{8F(1 + 2F)} \right) \right), \quad (19)$$

where $F = \frac{d^2}{A_R}$. It can be observed from (19) that the gain is a function of relative geometric quantities, i.e., the normalized (to the wavelength) transmit SIS' area A_T and the ratio F .

If one defines $G_T = \frac{A_T 4\pi}{\lambda^2}$ and $G_I = \frac{\lambda^2}{(4\pi d)^2}$, respectively, the gain of the transmit antenna, considered as aperture antenna, and the isotropic free-space channel gain, it turns out that the gain of the LIS is

$$G_R = \frac{g}{G_T G_I} = \frac{16\pi d^2}{3\lambda^2} \left(\frac{\sqrt{2F}}{\sqrt{1 + 2F}(1 + 4F)} + 2\text{acot} \left(\sqrt{8F(1 + 2F)} \right) \right), \quad (20)$$

which in general depends not only on the angle, as for antennas in the far-field, but also on the distance, i.e., on the relative position between transmitter and receiver.

It is interesting to analyze the behavior of (19) when the LIS is extremely large compared to the distance d (small F), that is

$$g^{(\text{large LIS})} = \frac{4\pi A_T}{3\lambda^2}, \quad (21)$$

which becomes independent of the distance. Instead, for large distances (large F), corresponding to the Fraunhofer far-field region, (19) gives

$$g^{(\text{large } d)} = \frac{A_T A_R}{\lambda^2 d^2}. \quad (22)$$

The latter is the result found by Miller [20] (reported in (15) with a different normalization factor) when considering thin volumes and it is nothing else than the well-known Friis' formula. In fact, setting $G_R = \frac{A_R 4\pi}{\lambda^2}$, the gain of the receive antenna considered as aperture antenna, it is $g^{(\text{large } d)} = G_T G_R G_I$ [18].

Equation (16) and, in particular, (18) and (19) represent simple design formula useful to characterize the link budget in LIS-based communications without resorting to e.m. extensive simulations.

IV. COMMUNICATION DoF BETWEEN INTELLIGENT SURFACES

In this section we derive approximate expressions for the communication DoF between a transmit SIS and a receive LIS antenna following 2D sampling theory arguments. The accuracy of such expressions with respect to the actual DoF value from the eigenfunction problem in Sec. II, is addressed in the numerical results.

With reference to Fig. 3, the wave originated by the point source \mathbf{s} has wavenumber k_0 in the radial direction $\mathbf{r} - \mathbf{s}$ between the point source and the generic point \mathbf{r} on the receive (observation) surface \mathcal{S}_R . Contrarily to what happens in 1D coordinate systems, where a linear transformation never changes or generates new frequency components, when moving to 2D and 3D coordinate systems, it may happen that the observed wavenumber is different from k_0 if the observation direction is different from $\mathbf{r} - \mathbf{s}$. More specifically, along the x and y directions of the receive surface, the observed wave is characterized by wavenumber

$$\mathbf{k}(\mathbf{r}, \mathbf{s}) = (k_x(\mathbf{r}, \mathbf{s}), k_y(\mathbf{r}, \mathbf{s}), 0) = \mathbf{r} - \mathbf{s} - \hat{\mathbf{n}}((\mathbf{r} - \mathbf{s}) \cdot \hat{\mathbf{n}}), \quad (23)$$

where $\hat{\mathbf{n}}$ is the unit vector perpendicular to the surface in the point \mathbf{r} , so that

$$\begin{aligned} k_x(\mathbf{r}, \mathbf{s}) &= k_0 \frac{r_x - s_x}{\sqrt{(r_x - s_x)^2 + (r_y - s_y)^2 + s_z^2}} \\ k_y(\mathbf{r}, \mathbf{s}) &= k_0 \frac{r_y - s_y}{\sqrt{(r_x - s_x)^2 + (r_y - s_y)^2 + s_z^2}}. \end{aligned} \quad (24)$$

Consider now an infinitesimal surface $d\mathbf{r}$ centered in \mathbf{r} . The received wave observed in \mathbf{r} can be seen as a two-dimensional signal whose local bandwidth changes slowly with $\mathbf{r} - \mathbf{s}$. The local bandwidth in the wavenumber domain observed in \mathbf{r} is the maximum wavenumber spread related to all point sources in \mathcal{S}_T . Specifically it is

$$B(\mathbf{r}) = \frac{1}{4} \text{area}_{\mathbf{s} \in \mathcal{S}_T} [\mathbf{k}(\mathbf{r}, \mathbf{s})] \quad (25)$$

where the operator $\text{area}_{\mathbf{s} \in \mathcal{S}_T}[\cdot]$ returns the area of the region in the complex plane spanned by the function $\mathbf{k}(\mathbf{r}, \mathbf{s})$ when parameter \mathbf{s} varies in \mathcal{S}_T .

Considering that the DoF (i.e., the number of requested samples at Nyquist rate) of a 2D signal of (spatial) bandwidth B in an area S is, as first order approximation, equal to $\frac{BS}{\pi^2}$, the number of dimensions of the signal "projected" onto \mathcal{S}_R results

$$D = \frac{1}{\pi^2} \int_{\mathcal{S}_R} B(\mathbf{r}) d\mathbf{r}. \quad (26)$$

In the next section we make (26) particular to some LIS configurations with the purpose to derive simple expression of the DoF and obtain some interesting insights. Such expressions can be of interest when planning a wireless network based on intelligent surfaces.

A. DoF of Communicating Parallel LIS and SIS

For parallel intelligent surfaces, a way to compute (25) is to approximate the curve delimiting $\text{area}_{\mathbf{s} \in \mathcal{S}_T} [\mathbf{k}(\mathbf{r}, \mathbf{s})]$ with a quadrilateral having vertices given by $k_x^{(i)}(\mathbf{r}) = k_x(\mathbf{r}, \mathbf{s}^{(i)})$, $k_y^{(i)}(\mathbf{r}) = k_y(\mathbf{r}, \mathbf{s}^{(i)})$, $i = 1, 2, \dots, 5$, with $\mathbf{s}^{(1)} = (x_0 - L_x/2, y_0 - L_y/2, d)$, $\mathbf{s}^{(2)} = (x_0 + L_x/2, y_0 - L_y/2, d)$, $\mathbf{s}^{(3)} = (x_0 - L_x/2, y_0 + L_y/2, d)$, $\mathbf{s}^{(4)} = (x_0 + L_x/2, y_0 + L_y/2, d)$, $\mathbf{s}^{(5)} = \mathbf{s}^{(1)}$, and then by applying the Gauss' formula

$$A(\mathbf{r}) \simeq \frac{1}{2} \left| \sum_{i=1}^4 \left(k_x^{(i)}(\mathbf{r}) k_y^{(i+1)}(\mathbf{r}) - k_x^{(i+1)}(\mathbf{r}) k_y^{(i)}(\mathbf{r}) \right) \right|. \quad (27)$$

From (25) and (26) it follows that

$$D^{\parallel} \simeq \frac{1}{4\pi^2} \int_{\mathcal{S}_R} A(\mathbf{r}) d\mathbf{r}. \quad (28)$$

Unfortunately, (28) does not admit a closed-form expression in general. However, even though it requires the evaluation of a two-folded integral, its numerical computation is very fast and does not pose any particular issue compared to the numerical complexity of the eigenfunction problem (5) and (6).

Nevertheless, it could be of interest to derive closed-form expressions of (28) for some significant cases. Specifically, since $L_x, L_y \ll d$, setting $x_0 = y_0 = 0$, (28) gives (details are reported in Appendix)

$$D^{\parallel} \simeq \frac{2L_x L_y}{\lambda^2} \left(\frac{S_x \tan^{-1} \left(\frac{S_y}{\sqrt{4d^2 + S_x^2}} \right)}{\sqrt{4d^2 + S_x^2}} + \frac{S_y \tan^{-1} \left(\frac{S_x}{\sqrt{4d^2 + S_y^2}} \right)}{\sqrt{4d^2 + S_y^2}} \right). \quad (29)$$

For large distances $d \gg S_x, S_y$, i.e., in the far-field region, it is

$$D_{\text{large}}^{\parallel} = \frac{A_T A_R}{\lambda^2 d^2}, \quad (30)$$

which gives (14) derived in [20].

The limit of (29) for $S_x, S_y \rightarrow \infty$, i.e., very large surfaces, is

$$D_{\text{asympt}}^{\parallel} = \frac{\pi L_x L_y}{\lambda^2} = \frac{\pi A_T}{\lambda^2}. \quad (31)$$

Equation (31) indicates that the maximum DoF depends only on the area of the transmit surface (normalized to the square half-wavelength), i.e., the area of the smallest of the 2 antennas, and it represents the ultimate DoF limit which is independent of the distance. This result is reminiscent of the DoF in MIMO systems when the channel matrix is full rank, i.e., in the presence of rich multipath [3]. Unfortunately, in LOS channel condition, the rank of the channel matrix is 1, and hence $D = 1$ (only beamforming gain is present). Instead, result (29) indicates that with LIS one can obtain DoF larger than 1 even in LOS. Having large DoF in LOS could significantly increase the link capacity, especially at millimeter waves or in THz band where the multipath is not rich or could be dominated by the LOS component.

B. DoF of Communicating Perpendicular LIS and SIS

Consider now a transmit surface along the plane xz with coordinates $\mathbf{s} = (s_x, y_0, s_z)$ and a perpendicular receive LIS at distance $d = s_z$ with coordinates $\mathbf{r} = (r_x, r_y, 0)$. The centers and sizes of the transmit and receive intelligent surfaces are, respectively, $\mathbf{s}_0 = (x_0, y_0, d)$, (L_x, L_z) and $(0, 0, 0)$, (S_x, S_y) . The corresponding areas are $A_T = L_x L_z$ and $A_R = S_x S_y$.

Following a similar approach as in Sec. IV-A, by setting $\mathbf{s}^{(1)} = (x_0 - L_x/2, y_0, d - L_z/2)$, $\mathbf{s}^{(2)} = (x_0 + L_x/2, y_0, d - L_z/2)$, $\mathbf{s}^{(3)} = (x_0 - L_x/2, y_0, d + L_z/2)$, $\mathbf{s}^{(4)} = (x_0 + L_x/2, y_0, d + L_z/2)$, it is

$$D^\perp \simeq \frac{k_0^2 L_x L_z}{2\pi^2 \sqrt{4d^2 + S_y^2}} \left(\sqrt{4d^2 + S_y^2} \cot^{-1} \left(\frac{2d}{S_x} \right) - 2d \tan^{-1} \left(\frac{S_x}{\sqrt{4d^2 + S_y^2}} \right) \right). \quad (32)$$

For large $d \gg S_x, S_y$ one gets

$$D_{\text{large}}^\perp = \frac{A_T A_R S_y}{4\lambda^2 d^3}, \quad (33)$$

which, compared to the similar expression (30) for parallel surfaces, denotes a dependence on the ratio S_y/d . Such a term contributes to increase the DoF when the LIS is tall and hence is capable to "see" better the horizontal transmit surface.

The limit of (32) for $S_x, S_y \rightarrow \infty$, i.e., very large surfaces, is

$$D_{\text{asympt}}^\perp = \frac{\pi A_T}{\lambda^2}, \quad (34)$$

that is, the same as parallel surfaces.

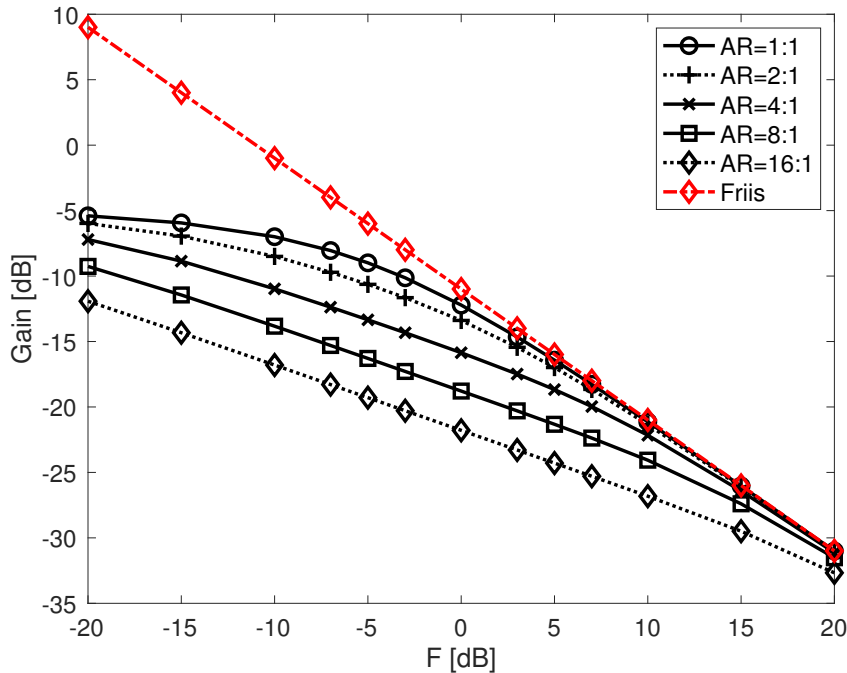


Fig. 4. Normalized gain vs $F = d^2/A_R$.

V. NUMERICAL RESULTS

In this section, we propose some numerical examples with the purpose to illustrate the potential advantages communications based on LIS and to assess the validity of the proposed method.

In Fig. 4 the total link gain between a SIS communicating with a LIS, normalized to the gain G_T of the transmit SIS, is shown as a function of F and for different values of the LIS' aspect ratio $AR = S_x : S_y$ using (18). Notice that this plot does not depend on λ and on the absolute distance between the intelligent surfaces and the dimension of the receive LIS, but only on the relative quantities $F = d^2/A_R$ and AR . When the size of the LIS is comparable or larger than the distance from the transmitter (small F), near-field effects become dominant leading to a saturation of the link gain toward the limit value (21). This can be ascribed to diffraction effects, which make the commonly used antenna aperture formula, according to which the antenna gain is proportional to the geometric area, no longer valid. From Fig. 4, it can be also noticed that the best geometric shape is the square one ($AR = 1 : 1$). For comparison, the gain obtained using the Friis' formula (22) is also shown from which it is evident it fails in modeling the link budget when LIS are used, especially for low F .

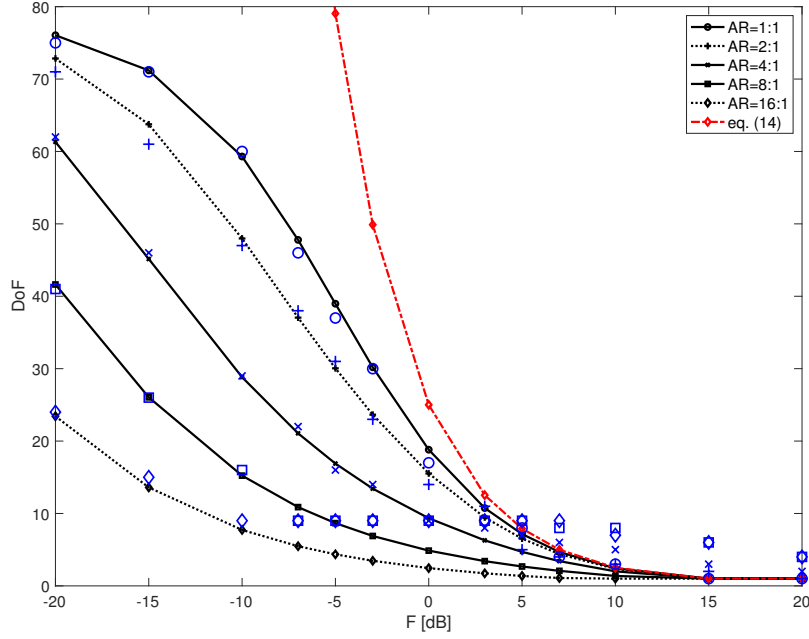


Fig. 5. DoF vs $F = d^2/A_R$ for parallel surfaces. $A_R = 25 \text{ cm}^2$, $f_c = 28 \text{ GHz}$.

Now we investigate the DoF available when a LIS and a SIS are communicating in the near and far field. Fig. 5 shows the DoF in (29) related to parallel surfaces as a function of F for different values of AR, with $\lambda = 1 \text{ cm}$ (28 GHz), and $5 \times 5 \text{ cm}^2$ LIS ($A_R = 25 \text{ cm}^2$).⁴

For low F (very large LIS), the DoF saturate to the limit value given by (31), in this case equal to 100. As the Fraunhofer far-field regime is approached (large F), the DoF tend to one as in conventional MIMO links in LOS condition, where only the beamforming gain is present. Again, the best LIS configuration is given by the square shape (AR = 1 : 1). The result obtained using (14) by [20] is also reported. It is evident how this expression, valid for antennas at distances much larger than their dimension, is not accurate for small F and it is not able to capture the effect of the aspect ratio of the LIS.

In order to validate the approach proposed in Sec. IV, results have been compared to those obtained by solving the eigenfunction problem in Sec. II. To this purpose, different numerical approximation methods exist (e.g., Galerkin's method) [21]. Among them, we considered the following one: we decomposed each surface in very small square patches of side $\Delta = \lambda/16$

⁴Although the values obtained from (29) should be rounded to the nearest integer value larger or equal to 1, here the continuous version is plotted to easy the reading.

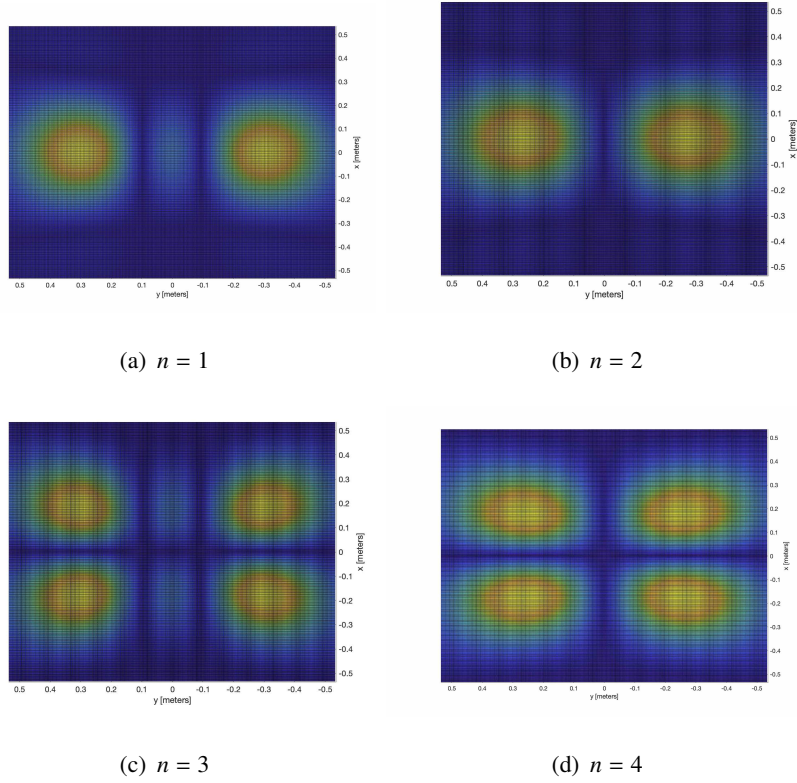


Fig. 6. Amplitude of the x -component of eigenfunctions $\psi_n(\mathbf{r})$ (receive LIS).

and we considered them as piece-wise constant basis functions for the surfaces. In this way the eigenfunction problem can be approximated into a singular value decomposition problem with dimension $A_R/\Delta^2 \times A_T/\Delta^2$. Unfortunately, such a method becomes intractable as soon as the surfaces become large compared to λ due to the corresponding huge dimension of the matrix to decompose. To make the computation affordable (a few days computation time), we considered a relative small LIS with $A_R = 1 \text{ m}^2$. The number of DoF has been computed by considering the largest eigenvalues within a tolerance of 3dB. Results are plotted in Fig. 5 (blue markers) and show a good agreement with the model developed in Sec. IV, especially for small F . For large F , there are some discrepancies, but the fact that our results are consistent with the analytical expression (14), which is accurate for large F , generates the suspect of numerical evaluation issues caused by the singular-value decomposition of huge matrices.

To get a qualitative idea about the shape of the base functions $\psi_n(\mathbf{r})$ and $\phi_n(\mathbf{r})$, in Figs. 6-9 the amplitude and phase of the x -component of basis functions $\{\psi_n(\mathbf{r})\}$, for $n = 1, 2, \dots, 4$, and $\{\phi_n(\mathbf{r})\}$, for $n = 1, 2$, are reported, respectively. For instance, Figs. 6a and 7a show the

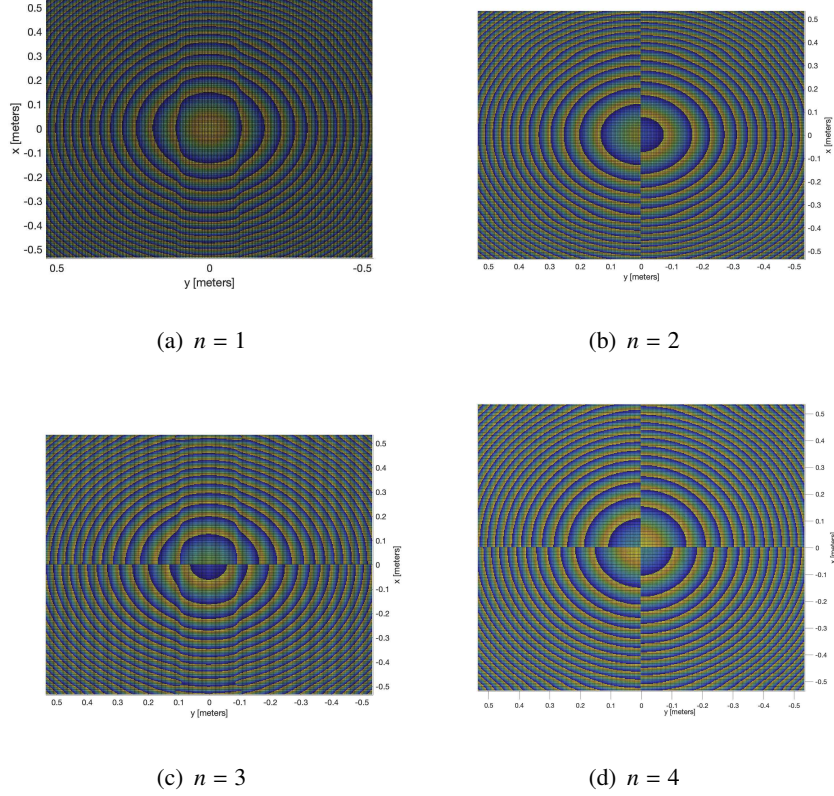


Fig. 7. Phase of the x -component of eigenfunctions $\psi_n(\mathbf{r})$ (receive LIS).

electrical field observed at the receive LIS when the exciting current $\phi_I(\mathbf{r})$, reported in Figs. 8a and 9a, is present. Notice that all functions are orthogonal.

The DoF for perpendicular surfaces, given by (32), is reported in Fig. 10 as a function of F for different values of AR under the same conditions as that of Fig. 5. As it can be noticed, the achievable DoF are less than that obtained for parallel surfaces, which represents the best geometric configuration to maximize the DoF. In this case the result in [20] reported in (14) is not applicable because it is not able to capture the DoF along the z direction of the SIS.

Interestingly, from the above results, it turns out that DoF significantly larger than 1 can be obtained at practical distances in LOS channel condition, which can have important implications. For instance, suppose a typical industrial scenario is considered, where a LIS of size $5 \times 5 \text{ m}^2$ is deployed on the factory ceiling at height $d = 5 \text{ m}$. From Fig. 5 it follows that the achievable DoF, supposing transmitting sensors equipped with SIS of area $A_T = 25 \text{ cm}^2$ located close to the floor, is $D \simeq 20$ ($F = 0 \text{ dB}$, $\text{AR} = 1 : 1$). This corresponds to a significant increase of link capacity with respect to the situation where only beamforming

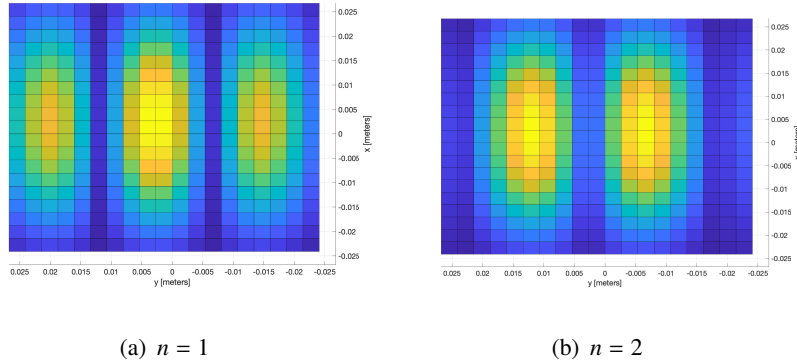


Fig. 8. Amplitude of the x -component of eigenfunctions $\phi_n(\mathbf{r})$ (transmit SIS).

gain is exploited and $\text{DoF} = 1$. For instance, using (12), the capacity gain at $\text{SNR} = 20$ dB is about 7.76.

This result can be interpreted also from another point of view: in fact, equivalently up to $D/A_T \simeq 8,000$ orthogonal links per square meter can be activated, which is very promising for the factories of the future where extremely high nodes density is expected. In addition, the possibility of making wireless links orthogonal at e.m. level, simplifies the channel multiple access, thus significantly reducing the communication latency.

VI. CONCLUSION

We have shown that the optimal communication between LIS/SIS can be formulated as an eigenfunction problem starting from e.m. arguments. Unfortunately, the numerical solution to the eigenfunction problem is prohibitive for LIS, so that simple but accurate analytical expressions for the DoFs and link gain have been derived. These expressions allow to get important insights about the communication between intelligent surfaces and can serve as design guidelines in future wireless networks employing LIS.

In particular, it has been shown that the achievable DoF and gain offered by the wireless link are determined only by geometric factors normalized to the wavelength, and that the classic Friis' formula is no longer valid in this scenario. The fundamental limits for very large intelligent surfaces have been found to be dependent only on the normalized area of the smallest antenna involved in the communication.

Furthermore, results indicate that when using LIS, contrarily to classic (massive) MIMO systems, one can exploit spatial multiplexing even in LOS (without multipath) at practical distances, which corresponds to a significant increase of spatial capacity density. In fact,

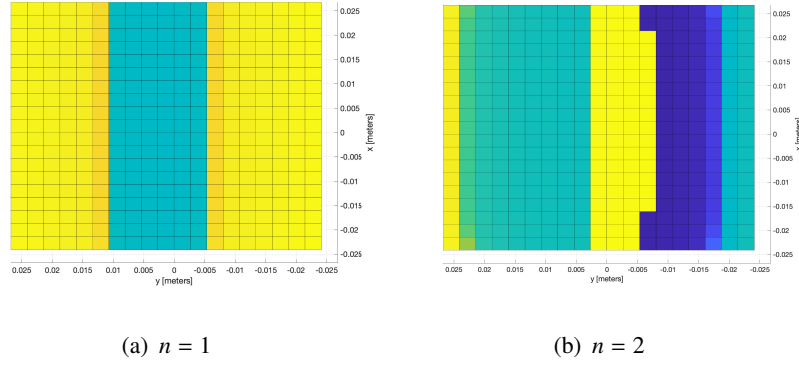


Fig. 9. Phase of the x -component of eigenfunctions $\phi_n(\mathbf{r})$ (transmit SIS).

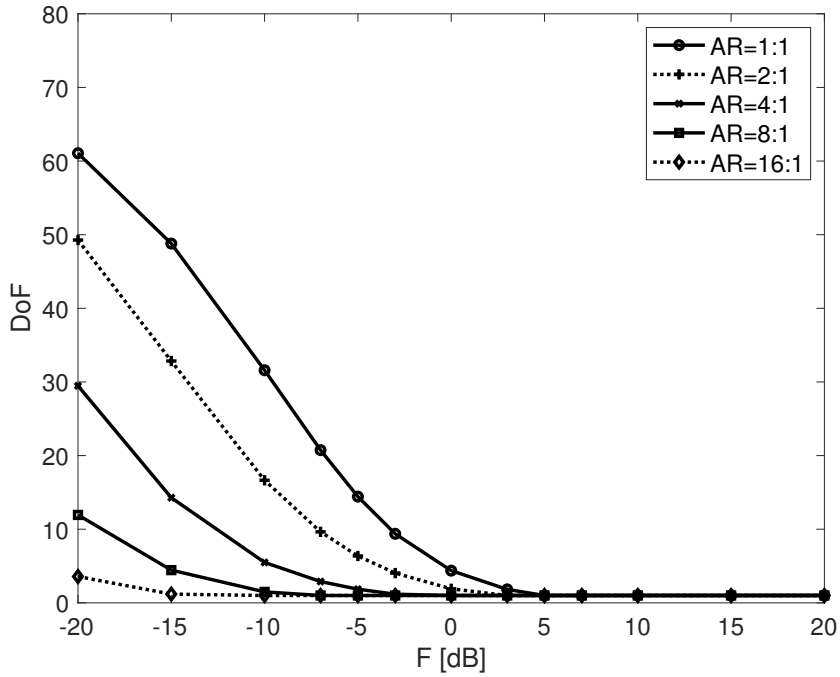


Fig. 10. DoF vs $F = d^2/A_R$ for perpendicular surfaces. $A_R = 25 \text{ cm}^2$, $f_c = 28 \text{ GHz}$.

using LIS, the ultimate wireless spatial channel capacity can be reached thus opening up the possibility of satisfying the challenging requirements of next generation wireless networks in terms of massive density and high capacity per square meter.

Obviously, several practical open issues need to be addressed before such limits can be approached by real systems.

APPENDIX A

In this Appendix, we show that

$$\sum_n \xi_n^2 = \int_{\mathcal{S}_R} \int_{\mathcal{S}_T} \|G(\mathbf{r} - \mathbf{s})\|^2 d\mathbf{r} d\mathbf{s}. \quad (35)$$

Specifically, since \mathcal{S}_T and \mathcal{S}_R are disjoint domains, tensor $G(\mathbf{r} - \mathbf{s})$ allows the bilinear expansion [14]

$$G(\mathbf{r} - \mathbf{s}) = \sum_n \xi_n \psi_n(\mathbf{r}) \otimes \phi_n^\dagger(\mathbf{s}). \quad (36)$$

The kj th element of tensor $G(\mathbf{r} - \mathbf{s})$ can be written as

$$\{G(\mathbf{r} - \mathbf{s})\}_{kj} = \sum_n \xi_n \{\psi_n(\mathbf{r})\}_k \cdot \{\phi_n^\dagger(\mathbf{s})\}_j, \quad (37)$$

then

$$|\{G(\mathbf{r} - \mathbf{s})\}_{kj}|^2 = \sum_n \sum_m \xi_n \xi_m \{\psi_n(\mathbf{r})\}_k \{\psi_m^\dagger(\mathbf{r})\}_k \{\phi_n^\dagger(\mathbf{s})\}_j \{\phi_m(\mathbf{s})\}_j. \quad (38)$$

For each k it is

$$\begin{aligned} \sum_{j=1}^3 |\{G(\mathbf{r} - \mathbf{s})\}_{kj}|^2 &= \sum_n \sum_m \xi_n \xi_m \{\psi_n(\mathbf{r})\}_k \{\psi_m^\dagger(\mathbf{r})\}_k \sum_{j=1}^3 \{\phi_n^\dagger(\mathbf{s})\}_j \{\phi_m(\mathbf{s})\}_j \\ &= \sum_n \sum_m \xi_n \xi_m \{\psi_n(\mathbf{r})\}_k \{\psi_m^\dagger(\mathbf{r})\}_k \phi_n^\dagger(\mathbf{s}) \phi_m(\mathbf{s}). \end{aligned} \quad (39)$$

By integrating in \mathcal{S}_T with respect to \mathbf{s} and thanks to the orthogonality condition (10), we obtain

$$\int_{\mathcal{S}_T} \sum_{j=1}^3 |\{G(\mathbf{r} - \mathbf{s})\}_{kj}|^2 d\mathbf{s} = \sum_n \xi_n^2 \{\psi_n(\mathbf{r})\}_k \{\psi_n^\dagger(\mathbf{r})\}_k. \quad (40)$$

From the previous result, it follows that

$$\begin{aligned} \int_{\mathcal{S}_T} \|G(\mathbf{r} - \mathbf{s})\|^2 d\mathbf{s} &= \int_{\mathcal{S}_T} \sum_{k=1}^3 \sum_{j=1}^3 |\{G(\mathbf{r} - \mathbf{s})\}_{kj}|^2 d\mathbf{s} \\ &= \sum_n \xi_n^2 \sum_{k=1}^3 \{\psi_n(\mathbf{r})\}_k \{\psi_n^\dagger(\mathbf{r})\}_k = \sum_n \xi_n^2 |\psi_n(\mathbf{r})|^2. \end{aligned} \quad (41)$$

By integrating (41) in \mathcal{S}_R and exploiting again the orthogonality condition (10), we obtain the final result (35).

APPENDIX B

Since $L_x, L_y \ll d$, setting $x_0 = y_0 = 0$, (28) can be expanded as

$$\begin{aligned}
D \simeq \frac{k_0^2}{8\pi^2} \int_{-S_x/2}^{S_x/2} \int_{-S_y/2}^{S_y/2} & - \frac{\left(r_x - \frac{L_x}{2}\right) \left(\frac{L_y}{2} + r_y\right)}{\sqrt{\left(\frac{L_y}{2} + r_y\right)^2 + \left(r_x - \frac{L_x}{2}\right)^2 + d^2} \sqrt{\left(\frac{L_x}{2} + r_x\right)^2 + \left(\frac{L_y}{2} + r_y\right)^2 + d^2}} \\
& + \frac{\left(\frac{L_x}{2} + r_x\right) \left(\frac{L_y}{2} + r_y\right)}{\sqrt{\left(\frac{L_x}{2} + r_x\right)^2 + \left(\frac{L_y}{2} + r_y\right)^2 + d^2} \sqrt{\left(\frac{L_y}{2} + r_y\right)^2 + \left(r_x - \frac{L_x}{2}\right)^2 + d^2}} \\
& - \frac{\left(r_x - \frac{L_x}{2}\right) \left(\frac{L_y}{2} + r_y\right)}{\sqrt{\left(r_x - \frac{L_x}{2}\right)^2 + \left(r_y - \frac{L_y}{2}\right)^2 + d^2} \sqrt{\left(\frac{L_y}{2} + r_y\right)^2 + \left(r_x - \frac{L_x}{2}\right)^2 + d^2}} \\
& + \frac{\left(\frac{L_y}{2} + r_y\right) \left(\frac{L_x}{2} + r_x\right)}{\sqrt{\left(\frac{L_x}{2} + r_x\right)^2 + \left(\frac{L_y}{2} + r_y\right)^2 + d^2} \sqrt{\left(\frac{L_x}{2} + r_x\right)^2 + \left(r_y - \frac{L_y}{2}\right)^2 + d^2}} \\
& - \frac{\left(\frac{L_x}{2} + r_x\right) \left(r_y - \frac{L_y}{2}\right)}{\sqrt{\left(\frac{L_x}{2} + r_x\right)^2 + \left(\frac{L_y}{2} + r_y\right)^2 + d^2} \sqrt{\left(\frac{L_x}{2} + r_x\right)^2 + \left(r_y - \frac{L_y}{2}\right)^2 + d^2}} \\
& + \frac{\left(r_y - \frac{L_y}{2}\right) \left(r_x - \frac{L_x}{2}\right)}{\sqrt{\left(\frac{L_x}{2} + r_x\right)^2 + \left(r_y - \frac{L_y}{2}\right)^2 + d^2} \sqrt{\left(r_x - \frac{L_x}{2}\right)^2 + \left(r_y - \frac{L_y}{2}\right)^2 + d^2}} \\
& + \frac{\left(r_x - \frac{L_x}{2}\right) \left(r_y - \frac{L_y}{2}\right)}{\sqrt{\left(\frac{L_y}{2} + r_y\right)^2 + \left(r_x - \frac{L_x}{2}\right)^2 + d^2} \sqrt{\left(r_x - \frac{L_x}{2}\right)^2 + \left(r_y - \frac{L_y}{2}\right)^2 + d^2}} \\
& - \frac{\left(\frac{L_x}{2} + r_x\right) \left(r_y - \frac{L_y}{2}\right)}{\sqrt{\left(\frac{L_x}{2} + r_x\right)^2 + \left(r_y - \frac{L_y}{2}\right)^2 + d^2} \sqrt{\left(r_x - \frac{L_x}{2}\right)^2 + \left(r_y - \frac{L_y}{2}\right)^2 + d^2}} dr_x dr_y. \tag{42}
\end{aligned}$$

The integrand of (42) can be approximated with the first-order Taylor double series expansion in L_x and L_y

$$\frac{2d^2 L_x L_y}{(d^2 + r_x^2 + r_y^2)^2} + O(L_x^2) + O(L_y^2), \tag{43}$$

resulting in

$$D \simeq \frac{d^2 L_x L_y}{\lambda^2} \int_{-S_x/2}^{S_x/2} \int_{-S_y/2}^{S_y/2} \frac{1}{(d^2 + r_x^2 + r_y^2)^2} dr_x dr_y \quad (44)$$

which admits a closed-form solution given by (29).⁵

REFERENCES

- [1] S. Vitturi, C. Zunino, and T. Sauter, "Industrial communication systems and their future challenges: Next-generation ethernet, IIoT, and 5G," *Proceedings of the IEEE*, vol. 107, no. 6, pp. 944–961, June 2019.
- [2] E. Björnson, L. Sanguinetti, H. Wymeersch, J. Hoydis, and T. L. Marzetta, "Massive MIMO is a reality - what is next?: Five promising research directions for antenna arrays," *Digital Signal Processing*, 2019. [Online]. Available: <http://www.sciencedirect.com/science/article/pii/S1051200419300776>
- [3] D. Tse and P. Viswanath, *Fundamentals of Wireless Communications*. New York, NY: Cambridge University Press, 2005.
- [4] A. Silva, F. Monticone, G. Castaldi, V. Galdi, A. Alù, and N. Engheta, "Performing mathematical operations with metamaterials," *Science*, vol. 343, no. 6167, pp. 160–163, 2014. [Online]. Available: <https://science.sciencemag.org/content/343/6167/160>
- [5] S. A. Tretyakov, "Metasurfaces for general transformations of electromagnetic fields," *Philosophical Transactions of the Royal Society A: Mathematical, Physical and Engineering Sciences*, vol. 373, Aug 2015. [Online]. Available: <https://doi.org/10.1098/rsta.2014.0362>
- [6] L. Di Palma, A. Clemente, L. Dussopt, R. Sauleau, P. Potier, and P. Pouliguen, "Circularly-polarized reconfigurable transmitarray in Ka-band with beam scanning and polarization switching capabilities," *IEEE Transactions on Antennas and Propagation*, vol. 65, no. 2, pp. 529–540, Feb 2017.
- [7] P. Nepa and A. Buffi, "Near-field-focused microwave antennas: Near-field shaping and implementation." *IEEE Antennas and Propagation Magazine*, vol. 59, no. 3, pp. 42–53, June 2017.
- [8] C. Liaskos, S. Nie, A. Tsiolaridou, A. Pitsillides, S. Ioannidis, and I. Akyildiz, "A new wireless communication paradigm through software-controlled metasurfaces," *IEEE Communications Magazine*, vol. 56, no. 9, pp. 162–169, Sep. 2018.
- [9] M. Di Renzo and J. Song, "Reflection probability in wireless networks with metasurface-coated environmental objects: an approach based on random spatial processes," *EURASIP Journal on Wireless Communications and Networking*, vol. 2019, no. 1, p. 99, Apr 2019. [Online]. Available: <https://doi.org/10.1186/s13638-019-1403-7>
- [10] M. D. Renzo, M. Debbah, D.-T. Phan-Huy, A. Zappone, M.-S. Alouini, C. Yuen, V. Sciancalepore, G. C. Alexandropoulos, J. Hoydis, H. Gacanin, J. d. Rosny, A. Bounceur, G. Lerosey, and M. Fink, "Smart radio environments empowered by reconfigurable AI meta-surfaces: an idea whose time has come," *EURASIP Journal on Wireless Communications and Networking*, vol. 2019, no. 1, p. 129, 2019. [Online]. Available: <https://doi.org/10.1186/s13638-019-1438-9>
- [11] L. Zhang, X. Q. Chen, S. Liu, Q. Zhang, J. Zhao, J. Y. Dai, G. D. Bai, X. Wan, Q. Cheng, G. Castaldi, V. Galdi, and T. J. Cui, "Space-time-coding digital metasurfaces," *Nature Communications*, vol. 9, no. 1, p. 4334, 2018. [Online]. Available: <https://doi.org/10.1038/s41467-018-06802-0>

⁵A closed-form expression can be derived also for the more general case of $x_0, y_0 \neq 0$, but it is not reported here due to space constraints.

- [12] S. Hu, F. Rusek, and O. Edfors, "Beyond massive MIMO: The potential of data transmission with large intelligent surfaces," *IEEE Transactions on Signal Processing*, vol. 66, no. 10, pp. 2746–2758, May 2018.
- [13] R. F. Harrington, *Time-Harmonic Electromagnetic Fields*. New York, USA: IEEE Press - Wiley, 2001.
- [14] M. Franceschetti, *Wave Theory of Information*. Cambridge, UK: Cambridge University press, 2018.
- [15] O. M. Bucci and G. Franceschetti, "On the degrees of freedom of scattered fields," *IEEE Transactions on Antennas and Propagation*, vol. 37, no. 7, pp. 918–926, July 1989.
- [16] M. Franceschetti, M. D. Migliore, and P. Minero, "The capacity of wireless networks: Information-theoretic and physical limits," *IEEE Trans. Inf. Theor.*, vol. 55, no. 8, pp. 3413–3424, Aug. 2009. [Online]. Available: <http://dx.doi.org/10.1109/TIT.2009.2023705>
- [17] M. Franceschetti, M. D. Migliore, P. Minero, and F. Schettino, "The degrees of freedom of wireless networks via cut-set integrals," *IEEE Transactions on Information Theory*, vol. 57, no. 5, pp. 3067–3079, May 2011.
- [18] C. A. Balanis, *Antenna Theory: analysis and design*. New Jersey, USA: Wiley, 2016.
- [19] A. S. Y. Poon, R. W. Brodersen, and D. N. C. Tse, "Degrees of freedom in multiple-antenna channels: a signal space approach," *IEEE Transactions on Information Theory*, vol. 51, no. 2, pp. 523–536, Feb 2005.
- [20] D. A. B. Miller, "Communicating with waves between volumes: evaluating orthogonal spatial channels and limits on coupling strengths," *Appl. Opt.*, vol. 39, no. 11, pp. 1681–1699, Apr 2000. [Online]. Available: <http://ao.osa.org/abstract.cfm?URI=ao-39-11-1681>
- [21] R. Piestun and D. A. B. Miller, "Electromagnetic degrees of freedom of an optical system," *J. Opt. Soc. Am. A*, vol. 17, no. 5, pp. 892–902, May 2000. [Online]. Available: <http://josaa.osa.org/abstract.cfm?URI=josaa-17-5-892>